

Molecular tests of the random phase approximation to the exchange-correlation energy functional

Filipp Furche*

Institut für Physikalische Chemie, Universität Karlsruhe, Kaiserstraße 12, 76128 Karlsruhe, Germany

(Received 29 May 2001; published 19 October 2001)

The exchange-correlation energy functional within the random phase approximation (RPA) is recast into an explicitly orbital-dependent form. A method to evaluate the functional in finite basis sets is introduced. The basis set dependence of the RPA correlation energy is analyzed. Extrapolation using large, correlation-consistent basis sets is essential for accurate estimates of RPA correlation energies. The potential energy curve of N_2 is discussed. The RPA is found to recover most of the strong static correlation at large bond distance. Atomization energies of main-group molecules are rather uniformly underestimated by the RPA. The method performs better than generalized-gradient-type approximations (GGA's) only for some electron-rich systems. However, the RPA functional is free of error cancellation between exchange and correlation, and behaves qualitatively correct in the high-density limit, as is demonstrated by the coupling strength decomposition of the atomization energy of F_2 . The GGA short-range correlation correction to the RPA by Yan, Perdew, and Kurth [Phys. Rev. B **61**, 16 430 (2000)] does not seem to improve atomization energies consistently.

DOI: 10.1103/PhysRevB.64.195120

PACS number(s): 71.15.Mb, 71.45.Gm, 31.10.+z, 31.25.-v

I. INTRODUCTION

Kohn-Sham (KS) density functional theory¹⁻³ is one of the most widely used methods in electronic structure theory. Due to a well-balanced compromise between accuracy and computational efficiency, generalized gradient approximations⁴⁻⁸ (GGA's) to the exchange-correlation energy functional are very successful in solid-state and particularly in molecular applications. However, further improvement of approximations to the exchange-correlation energy functional is still an issue. "Chemical accuracy" in atomization energies (1 kcal/mol) has not yet been achieved,⁹⁻¹³ energies and potentials are contaminated with self-interaction,¹⁴ and orbital energy spectra are qualitatively incorrect¹⁵⁻¹⁷—to name some of the most pressing difficulties of GGA-type functionals. Although these problems have been known for more than a decade, they are hard to overcome in a practicable and general manner.

An evident strategy for improvement is to identify the parts of the exchange-correlation energy for which the GGA is accurate and to treat the remainder exactly. For this purpose, the coupling strength decomposition of the exchange-correlation functional,¹⁸

$$E_{xc}[\rho] = \int_0^1 d\alpha W_\alpha[\rho], \quad (1)$$

has proved a convenient starting point. The integrand $W_\alpha[\rho]$ is defined as

$$W_\alpha[\rho] = \langle \Psi_\alpha[\rho] | \hat{W} | \Psi_\alpha[\rho] \rangle - \frac{1}{2} \int d^3r d^3r' \frac{\rho(\mathbf{r})\rho(\mathbf{r}')}{|\mathbf{r}-\mathbf{r}'|}, \quad (2)$$

where \hat{W} denotes the operator of the electron-electron Coulomb interaction, and $\Psi_\alpha[\rho]$ is the ground state of an N electron system with scaled interaction $\alpha\hat{W}$, whose ground-state density is constrained at the density ρ of the physical ground state $\Psi_1[\rho]$. For any approximate exchange-

correlation functional, the coupling strength decomposition can be computed by means of the scaling relation¹⁹⁻²¹

$$W_\alpha[\rho] = \frac{d}{d\alpha} (\alpha^2 E_{xc}[\rho_{1/\alpha}]), \quad (3)$$

where $\rho_\lambda(\mathbf{r}) = \lambda^3 \rho(\lambda\mathbf{r})$ is a scaled density, with uniform scaling parameter λ . Thus, W_α at $\alpha=0$ is determined by the high-density limit of E_{xc} , while the low-density limit corresponds to large α values. By construction, $\Psi_0[\rho]$ is the KS determinant, and $W_0[\rho] = E_x[\rho]$ is the exact orbital-dependent exchange functional.

For molecular densities, the GGA is known to yield a rather poor description of the high-density (exchange-only) limit. This is obvious, e.g., from the errors in GGA exchange-only (x-only) atomization energies that are significantly larger than errors in total GGA atomization energies.²² It is not sufficient to replace the GGA exchange part by the exact functional only, since there is considerable error cancellation between GGA exchange and correlation at small coupling constant values.²³ The random phase approximation (RPA) to the exchange-correlation functional^{18,24,25} is more accurate in the high-density limit. It correctly reduces to the exact exchange functional in the high-density limit, and the leading correlation contribution recovers the direct part of the exact high-density limit²⁰ of the correlation energy functional. $E_{xc}^{\text{RPA}}[\rho]$ is nonperturbative, containing contributions from all orders in α . It has a well-defined homogeneous limit and has played an important role in the development of homogeneous gas theory (for an overview, see Refs. 2 and 26).

Recently, there has been a revival of interest in the RPA.²⁷⁻²⁹ Yan, Perdew, and Kurth (YPK) have presented a GGA correction to RPA correlation $E_{c, \text{sr}}^{\text{GGA}}[\rho]$ (Ref. 30); it accounts for short-range correlation effects that are not well described within the RPA.³¹ YPK suggest that the GGA may be more accurate for the correction to the RPA than for the full exchange-correlation energy. In other words,

$$E_{xc}^{\text{RPA}+}[\rho] = E_{xc}^{\text{RPA}}[\rho] + E_{c, \text{sr}}^{\text{GGA}}[\rho] \quad (4)$$

is supposed to be a very accurate approximation to the exact exchange-correlation functional. YPK find that $E_{c,sr}^{\text{GGA}}[\rho]$ gives large corrections to total correlation energies but small corrections to atomization energies, and conclude that the RPA itself might come close to chemical accuracy.

Molecular tests of the RPA have been hampered by the fact that the common expression for $E_{xc}^{\text{RPA}}[\rho]$ [cf. Eq. (5) in Sec. II] contains the frequency-dependent RPA density response function of the interacting system at coupling strength α , which depends on the KS orbitals and the density in a complicated way. Moreover, a nontrivial integration over frequency is required. In Sec. II, the RPA correlation energy functional is recast into an explicitly orbital-dependent form which does not involve frequency integration [Eqs. (20) and (21) in Sec. II]. The derivation is simple and relies on the density-matrix-based approach to KS response theory.³² Implementation in finite basis sets is straightforward, as discussed in Sec. III. Technical details of the computations are given in Sec. IV. Due to the correlation cusp, the basis set dependence of the RPA correlation energy is quite different from that familiar from GGA calculations; this is investigated in a separate subsection. The first *ab initio* RPA results for atomization energies as well as bond properties of the N_2 molecule are presented in Sec. V. (The author is aware of similar work by Fuchs and Gonze being in progress.³³) The coupling strength dependence of the F_2 atomization energy within the GGA and the RPA is analyzed in detail. Conclusions are discussed in Sec. V.

II. THEORY

Following Langreth and Perdew,^{18,25} the coupling strength integrand W_α can be expressed as

$$W_\alpha = W_0 - \int_0^\infty \frac{d\omega}{2\pi} \text{Im} \int dx dx' \frac{\chi_\alpha(\omega, x, x') - \chi_0(\omega, x, x')}{|\mathbf{r} - \mathbf{r}'|}. \quad (5)$$

$\chi_\alpha(\omega)$ is the frequency-dependent density response function of the system with scaled interaction and fixed density, and $\chi_0(\omega)$ is the KS density response function. As usual, $x = (\mathbf{r}, \sigma)$ denotes a set of space-spin coordinates. Time-dependent Kohn-Sham (TDKS) theory leads to a Dyson-type equation for $\chi_\alpha(\omega)$,³⁴

$$\begin{aligned} \chi_\alpha(\omega, x, x') &= \chi_0(\omega, x, x') + \int dx dx_1 \chi_0(\omega, x, x_1) \\ &\times \left(\frac{\alpha}{|\mathbf{r}_1 - \mathbf{r}'_1|} + f_{xc\alpha}(\omega, x_1, x'_1) \right) \chi_\alpha(\omega, x'_1, x'). \end{aligned} \quad (6)$$

$f_{xc\alpha}(\omega)$ denotes the frequency-dependent exchange-correlation kernel at coupling strength α . The RPA coupling strength integrand W_α^{RPA} is obtained by replacing $\chi_\alpha(\omega)$ with its RPA counterpart $\chi_\alpha^{\text{RPA}}(\omega)$ in Eq. (5). $\chi_\alpha^{\text{RPA}}(\omega)$ is defined by¹⁸

$$\begin{aligned} \chi_\alpha^{\text{RPA}}(\omega, x, x') &= \chi_0(\omega, x, x') + \int dx_1 dx'_1 \chi_0(\omega, x, x_1) \\ &\times \frac{\alpha}{|\mathbf{r}_1 - \mathbf{r}'_1|} \chi_\alpha^{\text{RPA}}(\omega, x'_1, x'); \end{aligned} \quad (7)$$

i.e., $f_{xc\alpha}(\omega)$ in Eq. (6) is formally set to zero.

In the following it is shown how the calculation of W_α^{RPA} can be reduced to finite-dimensional linear algebra in finite basis sets. The procedure largely follows Ref. 32, to which the reader is referred for details. $\chi_\alpha^{\text{RPA}}(\omega)$ can be considered as the diagonal of the *density-matrix* response function $\Xi_\alpha^{\text{RPA}}(\omega)$,

$$\chi_\alpha^{\text{RPA}}(\omega, x, x') = \Xi_\alpha^{\text{RPA}}(\omega)(x, x, x', x'). \quad (8)$$

$\Xi_\alpha^{\text{RPA}}(\omega)$ is an operator on the Hilbert space $L = L_{\text{occ}} \otimes L_{\text{virt}} \oplus L_{\text{virt}} \otimes L_{\text{occ}}$, where L_{occ} and L_{virt} denote the Hilbert spaces of occupied and virtual KS molecular orbitals (MO's) associated with the ground-state density ρ . (Note that the density determines the KS potential and thus *all* MO's, occupied and virtual.) For vectors in L the notation

$$|X, Y\rangle = \begin{pmatrix} X \\ Y \end{pmatrix} \quad (9)$$

is convenient, i.e., $X \in L_{\text{occ}} \otimes L_{\text{virt}}$, $Y \in L_{\text{virt}} \otimes L_{\text{occ}}$. $\Xi_\alpha^{\text{RPA}}(\omega)$ has a straightforward matrix equivalent, in contrast to $\chi_\alpha^{\text{RPA}}(\omega)$. From the equation of motion for the TDKS density matrix it follows³² that $\Xi_\alpha^{\text{RPA}}(\omega)$ is related to the TDKS response operator within the RPA $\Lambda_\alpha^{\text{RPA}}$ by

$$\Xi_\alpha^{\text{RPA}}(z) = -(\Lambda_\alpha^{\text{RPA}} - \Delta z)^{-1}, \quad z \in \mathbb{C}. \quad (10)$$

$\Lambda_\alpha^{\text{RPA}}$ and Δ are defined on L and can be cast in the well-known form

$$\Lambda_\alpha^{\text{RPA}} = \begin{pmatrix} A_\alpha & B_\alpha \\ B_\alpha & A_\alpha \end{pmatrix}, \quad \Delta = \begin{pmatrix} 1 & 0 \\ 0 & -1 \end{pmatrix}. \quad (11)$$

Assuming real KS MO's, A_α and B_α are symmetric and have the matrix elements

$$(A_\alpha - B_\alpha)_{iajb} = (\epsilon_a - \epsilon_i) \delta_{ij} \delta_{ab}, \quad (12a)$$

$$(A_\alpha + B_\alpha)_{iajb} = (A_\alpha - B_\alpha)_{iajb} + 2\alpha \langle ij|ab \rangle. \quad (12b)$$

As usual, indices i, j, \dots label occupied and a, b, \dots virtual MO's; ϵ_i, ϵ_a are orbital energies and $\langle ij|ab \rangle$ is the matrix element of the electron-electron interaction (in Dirac notation). Equations (8) and (10) are generalizations of the Dyson-type equation (7). The matrix representation of $\Lambda_\alpha^{\text{RPA}}$ is the key to the basis set formulation of the RPA, since the matrix elements reduce to a finite number of standard molecular integrals in finite basis sets.

The integration over frequency in Eq. (5) can be carried out using the resolvent equation (10). The poles of $-\Xi_\alpha^{\text{RPA}}$ at positive frequency are the positive eigenvalues $\Omega_{n\alpha}^{\text{RPA}}$ of $\Lambda_\alpha^{\text{RPA}}$, and the residues are given by the corresponding eigen-

projectors $|X_{n\alpha}, Y_{n\alpha}\rangle\langle X_{n\alpha}, Y_{n\alpha}|$. This leads to the RPA eigenvalue problem^{32,35} at coupling strength α ,

$$(\Lambda_\alpha^{\text{RPA}} - \Omega_{n\alpha}\Delta)|X_{n\alpha}, Y_{n\alpha}\rangle = 0, \quad (13)$$

where the eigenvectors obey $\langle X_{n\alpha}, Y_{n\alpha}|\Delta|X_{n\alpha}, Y_{n\alpha}\rangle = 1$. Requiring that $\Xi_\alpha^{\text{RPA}}(z)$ be analytic in the upper half of the complex z plane, one arrives at

$$\int_0^\infty \frac{d\omega}{\pi} \text{Im} \Xi_\alpha^{\text{RPA}}(\omega) = - \sum_n |X_{n\alpha}, Y_{n\alpha}\rangle\langle X_{n\alpha}, Y_{n\alpha}|. \quad (14)$$

Using that Λ_0^{RPA} is diagonal, and inserting into Eqs. (8) and (5), the RPA coupling strength integrand takes the form

$$W_\alpha^{\text{RPA}} = W_0 + \frac{1}{2} \sum_{iajb} \langle ab|ij\rangle P_{\alpha iajb}, \quad (15)$$

where

$$P_{\alpha iajb} = \sum_n (X_{n\alpha} + Y_{n\alpha})_{ia} (X_{n\alpha} + Y_{n\alpha})_{jb} - \delta_{ij} \delta_{ab}. \quad (16)$$

The expression for P_α can be further simplified by the introduction of the one-component vectors³⁶

$$Z_{n\alpha} = \Omega_{n\alpha}^{1/2} (A_\alpha - B_\alpha)^{-1/2} (X_{n\alpha} + Y_{n\alpha}). \quad (17)$$

From Eq. (13) it follows that these vectors satisfy the symmetric eigenvalue equation

$$(M_\alpha - \Omega_{n\alpha}^2) Z_{n\alpha} = 0, \quad (18)$$

with the symmetric operator M_α given by

$$M_\alpha = (A_\alpha - B_\alpha)^{1/2} (A_\alpha + B_\alpha) (A_\alpha - B_\alpha)^{1/2}. \quad (19)$$

Eliminating $(X_{n\alpha} + Y_{n\alpha})$ by Eq. (17), and employing the spectral representation of M_α , P_α finally takes the form

$$P_\alpha = (A_\alpha - B_\alpha)^{1/2} M_\alpha^{-1/2} (A_\alpha - B_\alpha)^{1/2} - \mathbf{1}. \quad (20)$$

Inserting Eq. (15) into the adiabatic connection formula (1), the integrated RPA exchange-correlation energy follows as

$$E_{xc}^{\text{RPA}} = E_x + \frac{1}{2} \int_0^1 d\alpha \sum_{iajb} \langle ab|ij\rangle P_{\alpha iajb}. \quad (21)$$

Equations (20) and (21) express the RPA exchange-correlation energy as an explicit functional of the KS orbitals.

One can easily verify that the above expression has the behavior expected for the RPA to second order in the electron-electron interaction. Elementary perturbation theory starting from eigenvalue problem (18) yields

$$\begin{aligned} M_{\alpha iajb}^{-1/2} &= (\epsilon_a - \epsilon_i)^{-1/2} \\ &\times \left(\delta_{ij} \delta_{ab} - 2\alpha \frac{\langle ab|ij\rangle}{\epsilon_a + \epsilon_b - \epsilon_i - \epsilon_j} + O(\alpha^2) \right) \\ &\times (\epsilon_b - \epsilon_j)^{-1/2}. \end{aligned} \quad (22)$$

Thus, by Eqs. (20) and (15),

$$W_\alpha^{\text{RPA}} = W_0 - \alpha \sum_{iajb} \frac{\langle ab|ij\rangle^2}{\epsilon_a + \epsilon_b - \epsilon_i - \epsilon_j} + O(\alpha^2). \quad (23)$$

Upon coupling strength integration, the constant term gives the exchange functional, while the term linear in α produces the direct part of the exact second-order correlation energy functional.

There is obviously a close connection between the RPA exchange-correlation energy and time-dependent density functional theory (TDDFT). The eigenvalues $\Omega_{n\alpha}$ are excitation energies of a system with scaled electron interaction within the RPA, and the eigenvectors $|X_{n\alpha}, Y_{n\alpha}\rangle$ give the corresponding density changes.³² The expression for P_α , Eq. (16), may be viewed as a factorization of the correlation hole into contributions arising from collective excitations. This was actually the physical motivation behind the RPA as it was first introduced 50 years ago by Bohm and Pines.²⁴

In the derivation of Eq. (20) it has been tacitly assumed that $(A_\alpha - B_\alpha)$ and $(A_\alpha + B_\alpha)$ (and hence M_α) are positive definite. The positivity of $(A_\alpha - B_\alpha)$ is always given if the Aufbau principle is obeyed.³⁷ The same is true for $(A_\alpha + B_\alpha)$ in the RPA since the electron Coulomb interaction is positive as well, and coupling strengths α are always greater than or equal to zero. Without giving too much details the possibility should be mentioned here to define the RPA correlation energy in a Hartree-Fock (HF) context as well. The formalism largely has the same structure as above; merely $(A_\alpha - B_\alpha)$ and $(A_\alpha + B_\alpha)$ are replaced by the corresponding expressions familiar from time-dependent Hartree-Fock theory.³⁵ However, instabilities of the HF ground state showing up as negative eigenvalues of $(A_\alpha - B_\alpha)$ and $(A_\alpha + B_\alpha)$ can occur.³⁸ Moreover, although HF-based RPA correlation energies are exact to second order in the electron-electron interaction,³⁹ total correlation energies are considerably underestimated, as has been found in explorative calculations for the present work.

III. IMPLEMENTATION

Evaluation of the RPA correlation energy functional as given by Eqs. (20) and (21) was implemented in the second-order Møller-Plesset (MP2) module MPGRAD (Ref. 40) of the program system TURBOMOLE.⁴¹ The electron repulsion integrals $\langle ij|ab\rangle$ are constructed by transformation from the atomic orbital basis, a step which is routinely performed in MP2 calculations and has an asymptotic N^5 scaling of computational cost. The algorithm implemented in MPGRAD is integral direct; i.e., the integrals are transformed “on the fly,” making integral prescreening effective.⁴¹ Furthermore, molecular symmetry is fully exploited for finite point groups, so that only nonredundant integrals need to be calculated.⁴²

$M_\alpha^{-1/2}$ is obtained in a straightforward manner by diagonalization of M_α and taking the inverse square root of its eigenvalues, i.e.,

$$M_\alpha^{-1/2} = Z_\alpha \text{diag}(\Omega_{1\alpha}^{-1}, \Omega_{2\alpha}^{-1}, \dots) Z_\alpha^\dagger, \quad (24)$$

where Z_α signifies the matrix of eigenvectors. With an N^6 scaling, this is the most expensive step in RPA calculations even for smaller molecules with more than 20–30 electrons. However, the space L can be decomposed into a direct sum of subspaces transforming according to irreducible representations of the molecular point group. This is implemented by Clebsch-Gordan reduction of the representations spanned by direct products of occupied and virtual MO's. Since M_α is totally symmetric, the Wigner-Eckart theorem applies, and all operations need to be done for each irreducible subspace only. The cost for diagonalization thus reduces by approximately $1/g^3$, if g denotes the point group order. For most molecules treated below, this results in a speedup by a factor of 100–1000.

The coupling strength integral (21) is evaluated numerically. As the integrand is smooth and monotonous, this poses no particular difficulty. A seven-point Gauss-Legendre quadrature formula was found to produce energies accurate to at least six digits for several test cases. Correctness of the implementation was checked by comparison with RPA excitation energies from an independent TDDFT code³⁶ at $\alpha = 1$ and by numerical and analytical evaluation of $dW_\alpha^{\text{RPA}}/d\alpha|_{\alpha=0}$. Computation times for a single-point correlation energy ranged between seconds and a few minutes on a single CPU of a HP J240 workstation for most molecules considered below; they were considerably larger (several hours) due to the N^6 scaling for benzene and phenyl radical.

IV. COMPUTATIONAL DETAILS

All functionals were evaluated at self-consistent Perdew-Burke-Ernzerhof⁸ (PBE) GGA ground-state densities. The PBE parametrization was chosen since it does not contain empirically adjusted parameters and behaves reasonably under uniform scaling. Convergence of the density matrix to at least 10^{-7} was required, and fine quadrature grids (grid size 5⁴³) were used. The PBE and x-only calculations were performed with a modified version of the DSCF module^{41,43} of TURBOMOLE. Atomization energies were evaluated at the experimental structures taken from Ref. 44 for diatomics and from Ref. 10 for polyatomic molecules; for the H abstraction energy of benzene, structures were optimized using the PBE functional and a triple-zeta valence basis⁴⁵ with cc-pVTZ polarization functions (TZVPP). Except for this reaction, Dunning's correlation consistent basis sets were used throughout.^{46–48} The calculated atomization energies were corrected for basis set superposition error⁴⁹ (BSSE) according to the Boys-Bernardi counterpoise procedure.⁵⁰ RPA contributions to atomization energies were determined from the 45 extrapolated valence electron RPA correlation energies; the extrapolation method is discussed in Sec. V. PBE, x-only, and YPK short-range correction energies were evaluated in the cc-pV5Z basis. The bond distance and the harmonic frequency of N_2 were determined by numerical differentiation. For these properties as well as for the curves in Figs. 2 and 3, all-electron cc-pVQZ (Ref. 51) energies without BSSE correction were used. Experimental atomization energies of diatomics were calculated from spectroscopic D_0 values by subtraction of experimental zero-

TABLE I. Basis set dependence of the RPA valence electron correlation energy (hartree). PBE total energies are given for comparison.

Basis	$E_c(\text{RPA})$	$E(\text{PBE})$
cc-pVTZ	−0.550 874	−109.446 267
cc-pVQZ	−0.599 531	−109.455 091
cc-pV5Z	−0.621 644	−109.458 834
cc-pV6Z	−0.633 447	−109.459 781
34 extr.	−0.635 037	
45 extr.	−0.644 845	
56 extr.	−0.649 660	

point energies and anharmonicity corrections as available in Ref. 44. The experimental atomization energies of polyatomic molecules from Ref. 52 are based on thermochemical data, with calculated zero-point energies subtracted. The coupling strength decomposition of the PBE GGA as well as the YPK short-range correlation functional were obtained from scaling relation (3).

V. RESULTS

A. Basis set dependence

The dependence of the RPA correlation energy on the one-particle basis set is fundamentally different from that observed in local density approximation (LDA) and GGA calculations. This is exemplified for the N_2 molecule in Table I. Dunning's correlation consistent polarized valence electron basis sets cc-pVXZ, $X=3(\text{T}), 4(\text{Q}), 5, 6$, are designed for a systematic assessment of basis set effects.^{46–48} The number of polarization functions increases in a “correlation consistent” manner^{53,54} with the cardinal number X , i.e., $2d\ 1f$ for $X=3$, $3d\ 2f\ 1g$ for $X=4$, and so on. The largest basis set used here, cc-pV6Z, contains up to i ($l=6$) functions and a total of 210 primitive Gaussians per atom. While the PBE energy is converged to 10^{-3} Hartree in this basis, the error in the RPA correlation energy is still more than 10 times larger. The slow convergence with respect to the highest angular momentum quantum number in the atomic basis set used is not unexpected, since the correlation cusp⁵⁵ in the RPA pair density is expanded in a basis of MO products in the present method [see, e.g., Eq. (16)]. This implies that the RPA valence correlation energy depends on the cardinal number X as

$$E_c^{\text{RPA}}(X) = E_c^{\text{RPA}}(\infty) + A/X^3 \quad (25)$$

for sufficiently large X (Refs. 56–58); A is some constant. Equation (25) can be used to extrapolate the basis set limit $E_c^{\text{RPA}}(\infty)$, if E_c^{RPA} is known for two different cardinal numbers X, Y . This will be called XY extrapolation in the following.

In Fig. 1, the RPA valence electron correlation energy of N_2 is plotted as a function of the cardinal number X . In fact, an asymptotic X^{-3} dependence due to the correlation cusp is observed. The extrapolated energies converge more rapidly than the unextrapolated ones (Table I); the error in the 56

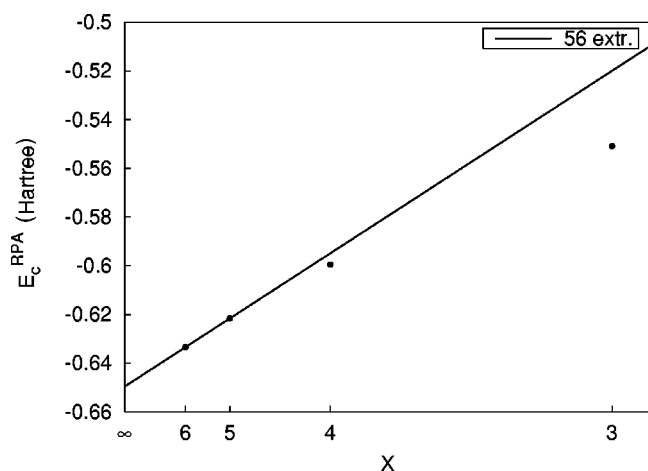


FIG. 1. Dependence of the RPA valence correlation energy E_c for N_2 on the cardinal number X of the basis set (X^{-3} scale). 56 extr. denotes a two-point extrapolation using $X=5$ and 6.

extrapolation is estimated to be less than or equal to 5 mhartree. This is still more than typical errors encountered for post-HF correlation methods.⁵⁸ A possible reason may be that PBE highest-occupied and lowest-unoccupied molecular orbital (HOMO-LUMO) gaps are much smaller than HF gaps, making response properties more sensitive to basis set changes.

The basis set convergence of RPA and PBE atomization energies of N_2 (Table II) is again strikingly different. While the PBE result is converged to about 1 kcal/mol at the cc-pVTZ level, the error in the RPA value is more than 12 kcal/mol. In fact, the unextrapolated RPA atomization energy is still more than 2 kcal/mol off the estimated basis set limit even in the cc-pV6Z basis. The extrapolated energies converge reasonably, though. The error in the 45 extrapolated RPA atomization energy is probably below 1 kcal/mol; the 45 extrapolation has therefore been used for the molecules in Table IV, below, as well. Experience with other methods⁵⁹ and explorative all-electron calculations indicate that errors due to the frozen-core approximation used in the RPA calculations are smaller than 1 kcal/mol. It is therefore estimated that the RPA and RPA+ atomization energies given in Table IV are accurate to about 1 kcal/mol compared to the all-electron basis set limit.

B. Properties of N_2

In Table III, PBE and RPA+ equilibrium bond lengths

TABLE II. Basis set dependence of calculated N_2 atomization energies (kcal/mol).

Basis	RPA	PBE
cc-pVTZ	210.8	242.8
cc-pVQZ	217.5	243.5
cc-pV5Z	220.2	243.6
cc-pV6Z	221.5	243.8
34 extr.	221.3	
45 extr.	222.7	
56 extr.	223.2	

TABLE III. Calculated bond length r_e and harmonic vibrational frequency ω_e of N_2 compared to experiment.

	RPA+	PBE	Expt. ^a
r_e (pm)	110.4	110.2	109.8
ω_e (cm^{-1})	2323	2349	2359

^aReference 44.

and harmonic vibrational frequencies of N_2 are compared to experiment. RPA results for these properties are nearly identical to RPA+ and are therefore not discussed separately here. Agreement of the PBE results with experiment is surprisingly good. The RPA+ results are slightly worse, but still close to PBE. Neglect of correlation generally gives too short bonds and too large frequencies; this is somewhat overcorrected by RPA+.

Potential energy curves of N_2 computed using the PBE, x-only, and RPA+ functionals are compared in Fig. 2. At large bond distance, the x-only curve exhibits artifacts well known from closed-shell HF theory. The PBE curve tends to a smaller value, indicating that the GGA incorporates part of the large static correlation in this limit. The RPA+ curve comes very close to zero. This is a remarkable behavior for a single-reference method,⁶⁰ since the huge error in the x-only energy is almost exactly canceled. At intermediate bond distance, the RPA+ curve has a spurious maximum. It cannot be decided at present if this is an intrinsic shortcoming of RPA+ or caused by a worsening of the PBE densities at long bond distance.

C. Atomization energies

In Table IV, calculated atomization energies of small main-group molecules are compared to experimental results. The present sample cannot claim statistical significance. The molecules in Table IV should rather be considered as individual, paradigmatic cases. By comparison with the x-only results it is evident that the RPA correlation energy recovers the main part of the correlation contribution to atomization

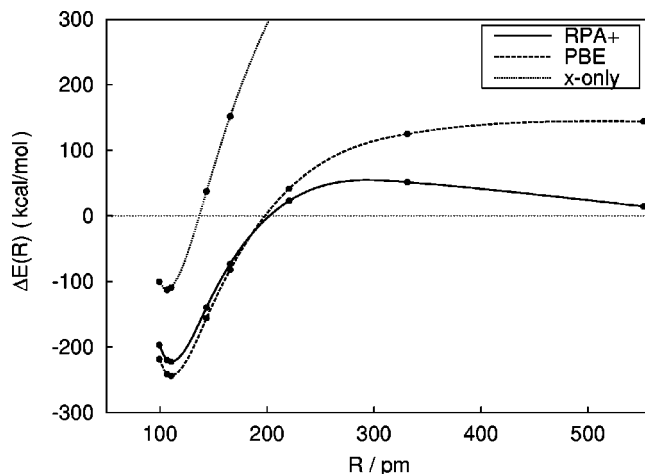


FIG. 2. Relative spin-restricted potential energy curves of N_2 . ΔE is the atomization energy, and R denotes the N-N distance.

TABLE IV. Calculated atomization energies (kcal/mol) compared to experiment. For details of the calculations see Sec. IV.

System	PBE	x-only	RPA	RPA+	Expt. ^a
H ₂	105	84	109	110	109
N ₂	244	111	223	223	228
O ₂	144	25	113	111	121
F ₂	53	-43	30	29	38
Ne ₂ ^b	0.11	-0.15	0.01	-0.08	0.08 ^c
Si ₂	81	38	70	70	75
HF	142	96	133	132	141
CO	269	170	244	242	259
CO ₂	416	234	364	360	389 ^d
C ₂ H ₂	415	291	381	378	405 ^d
H ₂ O	234	155	223	222	232 ^d
C ₆ H ₅ -H ^e	115	100	112	112	120 ± 1 ^f

^aReference 44, unless otherwise stated.

^bAll-electron results.

^cReference 65.

^dReference 52.

^eTZVPP basis, no counterpoise.

^fReference 61.

energies. However, except for H₂, RPA and RPA+ atomization energies are too small. Interestingly, this underestimation appears to be nearly independent of the error in the x-only atomization energies. For N₂, for example, the x-only atomization energy is smaller than half the experimental value, and the RPA is rather accurate, while it falls short for HF which is reasonably described in a single-determinant ansatz. For several “difficult” cases such as N₂, O₂, F₂, or CO₂, the RPA performs better than PBE, which tends to overestimate atomization energies of electron-rich compounds.¹¹ On the other hand, PBE results are clearly superior for HF, H₂O, or C₂H₂. Ne₂ is a typical dispersion-bound van der Waals molecule. In order to obtain meaningful results (BSSE not significantly larger than binding energies), all-electron calculations and special core-valence basis sets⁵¹ were used. As expected, the neon dimer is not bound in the x-only approximation; the PBE atomization energy is very close to the experimental result. Perhaps surprisingly, RPA+ fails, predicting a negative binding energy. As in all other cases except H₂ and N₂, the YPK short-range correlation correction has the wrong sign and does not improve the RPA result.

The hydrogen abstraction from benzene is a chemical reaction of interest in carbon chemistry and materials science; accurate theoretical predictions of the reaction energy are not easily achieved.⁶¹ The PBE reaction energy of 115 kcal/mol is about 5 kcal/mol too small compared to the experimental value. Again, the RPA result is even smaller. Due to the size of the molecule, a more economic basis set without extrapolation was used; however, it is estimated that RPA and RPA+ will still remain below the PBE reaction energy in the basis set limit.

In Fig. 3, the coupling strength decomposition of the correlation contribution to the atomization energy⁶² of F₂ ac-

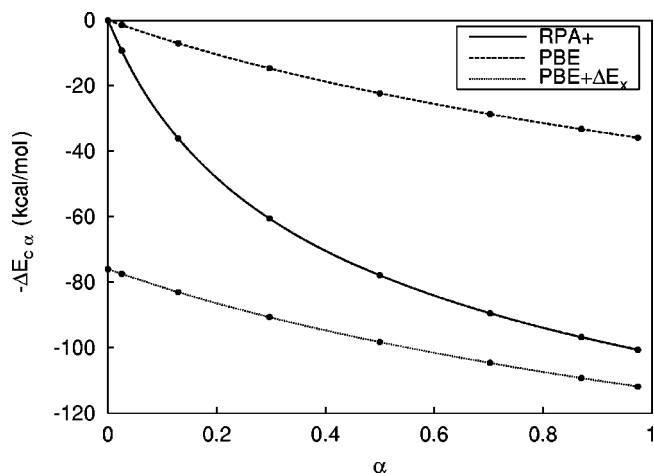


FIG. 3. Coupling strength decomposition of the correlation part ΔE_c of the F₂ atomization energy. ΔE_x denotes the x-only atomization energy.

ording to the adiabatic connection formula (1) is plotted. The total correlation part of the atomization energy is given by the positive area under the curves between $\alpha=0$ and 1. The plot illustrates well why GGA correlation functionals are not compatible with exact exchange: The PBE curve is much too flat for all coupling strength values. The PBE curve shifted by the difference between the x-only and PBE exchange atomization energies ΔE_x gives a better approximation to the total correlation part of the atomization energy. However, the shifted PBE curve is qualitatively in wrong in the small- α (high-density) limit, since it does not tend to zero. This has been identified as the main reason why GGA’s overestimate atomization energies of electron-rich molecules such as F₂.^{21,63} The RPA+ curve behaves qualitatively correct over the whole α range. The integral is still too small, however, as indicated by the underestimation of the total atomization energy.

VI. CONCLUSIONS

From the results presented above it is clear that neither RPA nor RPA+ reach chemical accuracy for atomization energies. The RPA is superior to the GGA only for certain electron-rich molecules where the GGA itself has substantial problems. This modest improvement has to be paid by a dramatic increase of computational cost. Clearly, RPA and RPA+ cannot (yet) compete with post-HF methods such as the coupled cluster singles and doubles approximation (CCSD), which give better results⁵⁹ at a comparable price. The present conclusions are somewhat limited by the accuracy of the PBE densities used. It is not expected that more accurate densities will alter the results dramatically, but a definite answer must be left to future investigations.

On the other hand, the RPA correlation energy seems to account well for strong static correlations. This is obvious from the potential energy curves (Fig. 2) and the fact that errors in RPA atomization energies of molecules such as N₂,

O₂, and F₂ are not significantly larger than for others. On the whole, the RPA performs still reasonably without error cancellation between (exact) exchange and correlation. This indicates that RPA correlation energies are more accurate than GGA correlation energies. Few other correlation energy functionals are known⁶⁴ that yield atomization energies of comparable quality when combined with exact exchange. It is surprising, though, that the YPK GGA corrections to atomization energies are not satisfactory. Further detailed studies are needed to understand this unexpected result.

ACKNOWLEDGMENTS

The author would like to thank R. Ahlrichs for advice and support, and J. P. Perdew for encouragement and helpful comments. Discussions with S. Kurth are acknowledged. This work was supported by the Deutsche Forschungsgemeinschaft, SFB 195 (“Lokalisierung von Elektronen in makroskopischen und mikroskopischen Systemen”). Financial support by the Studienstiftung des deutschen Volkes for a visit at Tulane University is also acknowledged.

*Electronic address: Filipp.Furche@chemie.uni-karlsruhe.de

¹W. Kohn and L.J. Sham, Phys. Rev. **140**, A1133 (1965).

²R.M. Dreizler and E.K.U. Gross, *Density Functional Theory* (Springer, Berlin, 1990).

³R.G. Parr and W. Wang, *Density-Functional Theory of Atoms and Molecules* (Oxford University Press, New York, 1989).

⁴J.P. Perdew, Phys. Rev. B **33**, 8822 (1986).

⁵C. Lee, W. Yang, and R.G. Parr, Phys. Rev. B **37**, 785 (1988).

⁶A.D. Becke, Phys. Rev. A **38**, 3098 (1988).

⁷A.D. Becke, J. Chem. Phys. **98**, 5648 (1993).

⁸J.P. Perdew, K. Burke, and M. Ernzerhof, Phys. Rev. Lett. **77**, 3865 (1996).

⁹J. Andzelm and E. Wimmer, J. Chem. Phys. **96**, 1280 (1992).

¹⁰B.G. Johnson, P.M.W. Gill, and J.A. Pople, J. Chem. Phys. **98**, 5612 (1993).

¹¹M. Ernzerhof and G.E. Scuseria, J. Chem. Phys. **110**, 5029 (1999).

¹²A.J. Cohen and N.C. Handy, Chem. Phys. Lett. **316**, 160 (2000).

¹³R. Ahlrichs, F. Furche, and S. Grimme, Chem. Phys. Lett. **325**, 317 (2000).

¹⁴J.P. Perdew and A. Zunger, Phys. Rev. B **23**, 5048 (1981).

¹⁵R. van Leeuwen, O.V. Gritsenko, and E.J. Baerends, Top. Curr. Chem. **180**, 107 (1995).

¹⁶M. Städele, J.A. Majewski, P. Vogl, and A. Görling, Phys. Rev. Lett. **79**, 2089 (1997).

¹⁷A. Görling, Phys. Rev. Lett. **83**, 5459 (1999).

¹⁸D.C. Langreth and J.P. Perdew, Solid State Commun. **17**, 1425 (1975).

¹⁹M. Levy and J.P. Perdew, in *Single-Particle Density in Physics and Chemistry*, edited by N.H. March and B.M. Deb (Academic, London, 1987), pp. 54–55.

²⁰A. Görling and M. Levy, Phys. Rev. B **47**, 13 105 (1993).

²¹M. Ernzerhof, Chem. Phys. Lett. **263**, 499 (1996).

²²S. Kurth, J.P. Perdew, and P. Blaha, Int. J. Quantum Chem. **75**, 889 (1999).

²³K. Burke, J.P. Perdew, and M. Ernzerhof, Int. J. Quantum Chem. **61**, 287 (1997).

²⁴D. Bohm and D. Pines, Phys. Rev. **82**, 625 (1951).

²⁵D.C. Langreth and J.P. Perdew, Phys. Rev. B **15**, 2884 (1977).

²⁶A.L. Fetter and J.D. Walecka, *Quantum Theory of Many-Particle Systems*, International Series in Pure and Applied Physics (MacGraw-Hill, New York, 1971).

²⁷J.M. Pitarke and A.G. Eguiluz, Phys. Rev. B **57**, 6329 (1998).

²⁸J.F. Dobson and J. Wang, Phys. Rev. Lett. **82**, 2123 (1999).

²⁹S. Kurth and J.P. Perdew, Phys. Rev. B **59**, 10 461 (1999).

³⁰Z. Yan, J.P. Perdew, and S. Kurth, Phys. Rev. B **61**, 16 430 (2000).

³¹K.S. Singwi, M.P. Tosi, R.H. Land, and A. Sjölander, Phys. Rev. **176**, 589 (1968).

³²F. Furche, J. Chem. Phys. **114**, 5982 (2001).

³³M. Fuchs and X. Gonze, Bull. Am. Phys. Soc. **46**, 1080 (2001).

³⁴E.K.U. Gross and W. Kohn, Adv. Quantum Chem. **21**, 255 (1990).

³⁵A.D. McLachlan and M.A. Ball, Rev. Mod. Phys. **36**, 844 (1964).

³⁶R. Bauernschmitt and R. Ahlrichs, Chem. Phys. Lett. **256**, 454 (1996).

³⁷R. Bauernschmitt and R. Ahlrichs, J. Chem. Phys. **104**, 9047 (1996).

³⁸J. Čížek and J. Paldus, J. Chem. Phys. **47**, 3976 (1967).

³⁹A. Szabo and N.S. Ostlund, J. Chem. Phys. **67**, 4351 (1977).

⁴⁰F. Haase and R. Ahlrichs, J. Comput. Chem. **14**, 907 (1993).

⁴¹R. Ahlrichs *et al.*, Chem. Phys. Lett. **162**, 165 (1989) (for the current version, see <http://www.chemie.uni-karlsruhe.de/PC/TheoChem>).

⁴²M. Häser, J. Almlöf, and M. Feyereisen, Theor. Chim. Acta **79**, 115 (1991).

⁴³O. Treutler and R. Ahlrichs, J. Chem. Phys. **102**, 346 (1995).

⁴⁴K.P. Huber and G. Herzberg, *Constants of Diatomic Molecules*, Vol. IV of *Molecular Spectra and Molecular Structure* (Van Nostrand Reinhold, New York, 1979).

⁴⁵A. Schäfer, C. Huber, and R. Ahlrichs, J. Chem. Phys. **100**, 5829 (1994).

⁴⁶T.H. Dunning, Jr., J. Chem. Phys. **90**, 1007 (1989).

⁴⁷D.E. Woon and T.H. Dunning, Jr., J. Chem. Phys. **98**, 1358 (1993).

⁴⁸A. Wilson, T. van Mourik, and T.H. Dunning, Jr., J. Mol. Struct.: THEOCHEM **388**, 339 (1997).

⁴⁹B.J. Ransil, J. Chem. Phys. **34**, 2109 (1961).

⁵⁰S.F. Boys and F. Bernardi, Mol. Phys. **19**, 553 (1970).

⁵¹D.E. Woon and T.H. Dunning, Jr., J. Chem. Phys. **103**, 4572 (1995).

⁵²C. Adamo, M. Ernzerhof, and G.E. Scuseria, J. Chem. Phys. **112**, 2643 (2000).

⁵³K. Jankowski *et al.*, J. Chem. Phys. **82**, 1413 (1984).

⁵⁴R. Ahlrichs, P. Scharf, and K. Jankowski, Chem. Phys. **98**, 381 (1985).

⁵⁵T. Kato, Commun. Pure Appl. Math. **10**, 151 (1957).

⁵⁶W. Kutzelnigg and J.D. Morgan III, J. Chem. Phys. **96**, 4484 (1992).

⁵⁷T. Helgaker, W. Klopper, H. Koch, and J. Noga, J. Chem. Phys. **106**, 9639 (1997).

⁵⁸A. Halkier *et al.*, Chem. Phys. Lett. **286**, 243 (1998).

⁵⁹K.L. Bak *et al.*, Chem. Phys. Lett. **317**, 116 (2000).

⁶⁰W. Chen and H.B. Schlegel, J. Chem. Phys. **101**, 5957 (1994).

⁶¹K. May *et al.*, Phys. Chem. Chem. Phys. **2**, 5084 (2000).

⁶²M. Ernzerhof, J.P. Perdew, and K. Burke, Int. J. Quantum Chem. **64**, 285 (1997).

⁶³A.D. Becke, J. Chem. Phys. **98**, 1372 (1993).

⁶⁴M. Seidl, J.P. Perdew, and S. Kurth, Phys. Rev. Lett. **84**, 5070 (2000).

⁶⁵J.F. Oglivie and F.Y.H. Wang, J. Mol. Struct. **273**, 277 (1992).